Advanced Modeling of Fluid Catalytic Cracking Riser-Type Reactors

K. N. Theologos and N. C. Markatos
Dept. of Chemical Engineering, National Technical University of Athens, Athens GR-157 73, Greece

A mathematical model is developed that predicts three-dimensional, two-phase-flow, heat transfer and reaction inside catalytic cracking riser-type reactors. The model consists of the full set of partial-differential equations that describe the conservation of mass, momentum, energy and chemical species for both phases in the reactor, coupled with empirical correlations concerning interphase friction, interphase heat-transfer and fluid-to-wall frictional forces. The cracking reaction is simulated by a simple three-lump kinetic model, but more realistic kinetic models can be easily included. The model can predict the most important engineering aspects of a riser reactor including pressure drop, catalyst holdup, interphase slip velocity, catalyst acceleration zone, choking behavior and temperature distribution in both phases, and yields distribution all over the reactor. It can also predict other complex engineering three-dimensional, two-phase problems realistically using computational fluid dynamics techniques.

Introduction

Fluid Catalytic Cracking (FCC) is an industrial operation that converts heavy hydrocarbons to lower molecular-weight products. Both the catalytic cracking reaction and the catalyst regeneration are carried out in fluidized beds. The development of new, very active cracking catalysts allowed the cracking reaction to be completed in short-contact-time riser reactors.

In a riser reactor the catalyst is pneumatically conveyed by the hydrocarbon vapors from the bottom to the top of a vertical lift line. During this conveying process the catalytic cracking reaction is completed through the efficient contact of the catalyst with the hydrocarbons.

The inlet zone of the riser reactor, where the catalyst is accelerating, is the most complex part of the reactor, where intense turbulence and flow inhomogeneities result in high temperature and concentration gradients. The hot spots appearing at the inlet zone of a riser reactor promote secondary cracking reactions that produce undesirable light hydrocarbons and coke (McKetta, 1981; Yen et al., 1985; Mauleon and Courcelle, 1985). The feed injection may control the flow of catalyst and hydrocarbons, to establish plug flow conditions in order to minimize the undesirable temperature gradients.

The overall performance of a riser reactor can be predicted using simple one-dimensional mass, energy and chemical species balances. This simple approach, however, cannot be applied over the inlet zone of a riser reactor, for the above reasons.

In the present study, a three-dimensional, two-phase mathematical model for simulating the flow, heat transfer and chemical reactions in a riser reactor is developed. This model and its solution algorithm are applied to study the process behavior in a typical riser reactor, especially over its complex inlet zone.

The model, that recognizes two phases (that is, the catalyst and the hydrocarbons), can predict the catalyst acceleration, heat transfer between the two phases and chemical reaction; and it can also evaluate the effect of the injection geometry on the above mentioned processes.

Physical and Mathematical Model

The proposed model considers two phases, the solid catalyst and the vapor hydrocarbons. It predicts the flow, temperature and concentration fields of both phases, as well as the local interphase slip velocity and other interesting process characteristics, all over the reactor. The full set of partial-differential equations governing the three-dimensional, two-phase-flow heat and mass transfer with chemical reaction is used. Interphase heat and momentum transfer are accounted for. Finite-

domain equations are derived by integration of the differential equations over control volumes that taken together fully cover the domain of interest and then are solved by an iterative procedure.

The governing differential equations

The starting point of the analysis is the set of elliptic, partial-differential equations that express the conservation of mass, momentum and energy in steady (and transient) three-dimensional and two-phase flows (Markatos and Moult, 1979; Spalding, 1981; Markatos, 1986). The independent variables of the problem are the three components (θ, r, z) of a polar-cylindrical coordinate system and time (t). The main dependent variables are:

- Volume fractions of hydrocarbons and catalyst, R_g and R_p.
- Gas and particles angular momentum, radial and axial velocities, $(ur)_g$, v_g, w_g, $(ur)_p$, v_p, w_p.
- Pressure, p, assumed the same for both phases.
- Specific enthalpies of gas and particles, h_g and h_p.
- Concentration of chemical species i, y_i, in the gaseous phase.

The governing partial-differential equations for all variables can be expressed in the following general form:

$$\frac{\partial}{\partial t}(R_i\rho_i\varphi)+\frac{1}{r}\frac{\partial}{\partial r}(rR_i\rho_i v_i\varphi)+\frac{1}{r}\frac{\partial}{\partial\theta}(R_i\rho_i u_i\varphi)+\frac{\partial}{\partial z}(R_i\rho_i w_i\varphi)$$
$$=\frac{1}{r}\frac{\partial}{\partial r}\left(rR_i\Gamma_\varphi\frac{\partial\varphi}{\partial r}\right)+\frac{1}{r}\frac{\partial}{\partial\theta}\left(R_i\Gamma_\varphi\frac{\partial\varphi}{r\partial\theta}\right)+\frac{\partial}{\partial z}\left(R_i\Gamma_\varphi\frac{\partial\varphi}{\partial z}\right)+S_\varphi \tag{1}$$

where φ is the dependent variable, Γ_φ and S_φ are diffusion coefficients and source terms per unit volume for variable φ, and subscript i refers to the phase in question (gaseous, g and particulate, p).

For the dependent variables R_g and R_p, $\varphi = 1$ and Eqs. 1 become the phase-continuity equations. For modeling the steady-state operation of a riser reactor, assuming a three-lump reaction scheme, 13 differential equations must be solved for six velocity components, pressure, two volume fractions, two enthalpies and two concentrations. The diffusion coefficients, Γ_φ, in Eqs. 1 are calculated as follows:

- For the solid-phase variables $\Gamma_\varphi = 0$, that is, diffusion fluxes are considered to be zero for the noncontinuous (particulate) phase. This is not a limitation of the present model and any appropriate expression can be used. The zero value is assumed in the absence of any reliable experimental information.
- For u_g, v_g and w_g,

$$\Gamma_\varphi=\mu_{\text{eff}}=\mu_l+\mu_t$$

where μ_l and μ_t are the laminar and turbulence viscosity of the gaseous phase. For the purposes of this study and in the absence of any reliable two-phase turbulence model, it is assumed that $\mu_t = 1{,}000\ \mu_l$, but further research should be carried out on modeling the turbulence stress terms. In further work a standard $k\sim\epsilon$ model may be used (for example, Launder and Spalding, 1972; Markatos, 1986).

- For the other variables,

$$\Gamma_\varphi=\mu_l/\sigma_{l,\varphi}+\mu_t/\sigma_{t,\varphi}$$

where $\sigma_{l,\varphi}$ and $\sigma_{t,\varphi}$ are the laminar and turbulence Prandtl numbers for the variable φ. $\sigma_{t,\varphi}$ is taken as unity, a reasonable assumption.

Table 1. Source Terms in Differential Eqs. 1

φ	$\int S_\varphi d$ Vol (Source Term for the Computational Cell of Volume V)
w_g	$VR_g(-\rho_g g-\partial p/\partial z)+C_{f,ip}(w_p-w_g)$ + viscous terms
w_p	$VR_p(-\rho_p g-\partial p/\partial z)+C_{f,ip}(w_g-w_p)$
v_g	$VR_g(\rho_g u_g^2/r-\partial p/\partial r)+C_{f,ip}(v_p-v_g)$ + viscous terms
v_p	$VR_p(\rho_p u_p^2/r-\partial p/\partial r)+C_{f,ip}(v_g-v_p)$
$u_g r$	$C_{f,ip}r(u_p-u_g)$ + viscous terms
$u_p r$	$C_{f,ip}r(u_g-u_p)$
h_g	q_{pg}
h_p	$-q_{pg}$
y_1	$-R_0$
y_2	R_1-R_2

The source terms in Eq. 1 are given in Table 1. The sources are given in the form they appear in the finite-domain equations, that is, as the integral over a control volume. For the solution of the above set of partial-differential equations, it is assumed that both phases share the same pressure, p; and use is made of the additional equation:

$$R_g+R_p=1 \tag{2}$$

Phase interaction processes

The phase interaction processes are described by empirical algebraic equations. From these equations additional source terms are calculated and added in the appropriate differential equation.

Interphase friction

In vertical pneumatic conveying a drag force is exerted on the particles from the carrier gas, while an opposite force is exerted from the particles on the gas. This force controls the slip velocity between the two phases, the acceleration length of the particulate phase and the void fraction all over the conveying line. The interphase friction enters directly into the momentum equations.

The frictional force per unit volume at the gas-particle interphase due to differing phase velocities is calculated by the following expression (Markatos and Shinghal, 1982):

$$F=0.5C_D A_{pr}\rho_g|V_g-V_p|(V_g-V_p)=C_{f,ip}(V_g-V_p) \tag{3}$$

where:

A_{pr} = total projected area of particles per unit volume
V_g = gaseous phase velocity
V_p = particulate phase velocity

C_D = interphase friction coefficient between the two phases
ρ_g = density of gaseous phase

The projected area per unit volume, A_{pr}, assuming spherical particles, is calculated by the expression:

$$A_{pr} = 1.5R_p/d_p \tag{4}$$

where d_p is the particles' diameter.

The empirical correlation used for C_D (Lapple, 1950) is:

$$C_D = 24/Re_p(1 + 0.1667Re_p^{2/3}) \tag{5}$$

where Re_p, the particle Reynolds number, is calculated by:

$$Re_p = (d_p\rho_g/\mu_g)\,|\overline{V}_g - \overline{V}_p| \tag{6}$$

where $\overline{V}$ denotes resultant velocity.

To take into account the effect of local particle concentration of particles in fluidization, Richardson and Zaki (1954) showed that the drag force per unit volume of particles in mixtures of fluid and spherical particles can be expressed as:

$$F_D = 3/4C_D \frac{\rho_g(w_g - w_p)^2}{d_p} \epsilon^{-2.65} \tag{7}$$

where ϵ is the void fraction. This expression gives approximately the same results with Eq. 3 when applied to dilute-phase vertical pneumatic conveying.

Interphase heat transfer

Interphase heat transfer plays an important role in the catalytic cracking of hydrocarbons, especially in a riser-type reactor. In a conventional design, hot regenerated catalyst enters at the bottom of the riser as a dense bed, comes into contact with the gas-oil feed and gets accelerated by the gas-oil fraction that vaporizes. The rate of interphase heat transfer enters as an additional source/sink term in the energy differential equation is solved for each phase. Interphase heat transfer per unit volume is calculated by:

$$q_{pg} = h_{pg}A_{\text{int}}(T_p - T_g) \tag{8}$$

where h_{pg} is the heat-transfer coefficient between the two phases, A_{int} is the interphase area per unit volume and T_g and T_p are the hydrocarbon and catalyst temperatures, respectively.

The interphase heat-transfer coefficient, h_{pg}, is calculated from the following empirical correlation (Kunii and Levenspiel, 1969):

$$Nu_p = 0.03Re_p^{1.3} \quad 0.1 < \text{Re}_p < 100 \tag{9}$$

where the Nusselt number, Nu_p, is calculated by:

$$Nu_p = h_{pg}d_p/k_g \tag{10}$$

where k_g is the gas conductivity and the Reynolds number, Re_p, is calculated from Eq. 6.

The previously mentioned determination of the interphase heat-transfer coefficient correlates the rate of heat exchange between the two phases with the interphase slip velocity, which is important, especially over the acceleration zone at the bottom of the riser reactor.

Wall friction

The frictional force between the wall and the gas-solid suspension is assumed to be separated into two terms due, separately, to the fluid alone and to the effect of solid particles. The frictional pressure drop due to conveying the fluid alone in a pipe of length L and diameter D is defined by Fanning's equation:

$$\Delta P_{Fg} = \frac{f_g\rho_g w_g^2 L}{2D} \tag{11}$$

Assuming a smooth pipe, the friction factor f_g can be obtained by the empirical Blassius formula:

$$f_g = 0.316Re^{-1/4} \tag{12}$$

The wall friction due to solid particles can be calculated, following Fanning's equation (Yang, 1978), by:

$$\Delta P_{Fs} = \frac{f_p\rho_p(1-\epsilon)w_p^2 L}{2D} \tag{13}$$

The frictional factor, fp, is calculated by:

$$f_p\epsilon^3/(1-\epsilon) = \begin{cases} 0.0126[(1-\epsilon)Re_t/Re_p]^{-0.979} & V_g/V_t > 1.5 \\ 0.0410[(1-\epsilon)Re_t/Re_p]^{-1.021} & V_g/V_t < 1.5 \end{cases} \tag{14}$$

where V_g is the gas superficial velocity, V_t is the particle terminal (free-fall) velocity and Re_t is the terminal velocity Reynolds number.

The catalytic cracking reaction

The catalytic cracking of petroleum gas-oil results in a broad spectrum of products ranging from hydrogen and methane to heavy polymeric material adhering to the catalyst as coke. To describe the catalytic cracking reactions, the simple Weekman and Nace kinetics scheme (1970) was applied in the present work. This scheme was chosen for the sake of simplicity and computational economy and does not represent a limitation of the present model. More realistic schemes, of any complexity can be easily incorporated in future more detailed studies. The above scheme reduces the broad spectrum of catalytic cracking charge stocks and products into a three-component system, namely, the original charge material, the gasoline boiling fraction and the remaining C_4's (dry gas and coke).

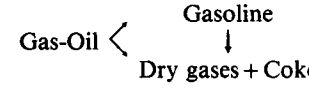

According to this reaction scheme the gas-oil feed is converted to gasoline and dry gases plus coke, while a part of gasoline is also converted to dry gases plus coke.

Gas-oil cracking can be represented by a second-order reaction with rate calculated by:

$$R_0 = k_0 \Phi y_1^2 \tag{15}$$

Gasoline formation can be represented by a second-order reaction with rate calculated by:

$$R_1 = k_1 \Phi y_1^2 \tag{16}$$

A first-order reaction is assumed for gasoline cracking. The rate of reaction is calculated by:

$$R_2 = k_2 \Phi y_2 \tag{17}$$

In the above set of equations y_1 and y_2 are the gas-oil and gasoline mass fractions, respectively.

The decay of catalyst due to coke formation on its surface is represented by the decay function Φ, that is related to the catalyst residence time t_c by:

$$\Phi = \frac{1}{t_c^n} \tag{18}$$

The kinetic parameters k_o, k_2 and n are related to the gas-phase temperature by Arrhenius equation.

As already mentioned above, even though there exist in the literature more realistic kinetic models that describe the cracking reactions using more detailed schemes, the Weekman and Nace model was selected because:

- It is still capable to illustrate the interactions between the process variables and the reaction rate and catalyst decay velocity.
- It predicts gasoline selectivity that represents the most significant contribution to the profitability of a catalytic cracking reactor.
- A simplified reaction scheme can perfectly illustrate the capabilities of computational fluid dynamics techniques in modeling complex process operations, within acceptable computational costs.

Finite-domain equations: numerical solution

To solve the partial-differential Eqs. 1 a numerical procedure is used. The domain of interest is covered by a grid that discretizes the continuous space into a number of control volumes or cells. The conventional "staggered" grid arrangement proposed by Patankar and Spalding (1972) is used. This means that the velocity components are calculated at the middle of the computational cell faces to which they are normal; all other variables are calculated at the center of the computational cells. The differential Eqs. 1 are integrated over the control volumes to yield the corresponding finite-domain equations.

These equations are solved using the SIMPLEST (Spalding, 1980) and IPSA (Spalding, 1977) algorithms that are embodied in the PHOENICS computer program (Spalding, 1981). The integration proceeds along the axis of the riser reactor from the inlet to the exit, and is repeated until convergence is achieved. More details may be found in, for example, Markatos (1989).

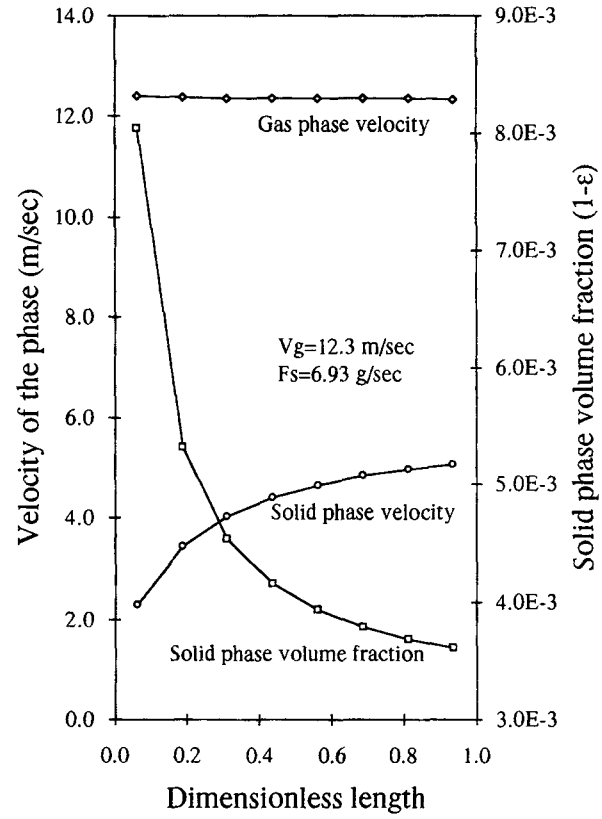

Figure 1. Typical predictions of solid-phase volume fraction and phase velocities.

Model capabilities and simplifications

The proposed modeling technique can predict the most important engineering aspects of a riser catalytic cracking reactor, including: pressure drop, catalyst holdup, interphase slip velocity, catalyst acceleration zone, choking behavior, temperature distribution of both phases, and yields distribution all over the reactor.

Two simplifications have been introduced in the present work. First, a simple kinetic model (the three-lump Weekman and Nace model, 1970) was used in order to describe the catalytic cracking reactions. Since 1970 more detailed kinetic models have been presented in the literature (for example, the ten-lump Jacob et al. model, 1976) that describe more realistically the cracking reactions. The reasons for this simplification have been given above.

Second, the presence of both a gaseous and a liquid hydrocarbon fraction at the bottom of the riser was not accounted for. In reality, the gas-oil vaporizes gradually inside the reactor as it comes into contact with the hot regenerated catalyst. Full treatment of this process would necessitate the solution of a three-phase problem.

These two simplifications do not represent limitations of the proposed modeling procedure. The aim of the study is mainly to illustrate a novel approach to riser reactor design and to predict the hydrodynamics effects on the operation of multinozzle riser reactors. Research is currently in progress to incorporate a more detailed lumping and reaction scheme, and to compute the gradual vaporization of gas-oil. To illustrate the above mentioned capabilities of the model, one-dimen-

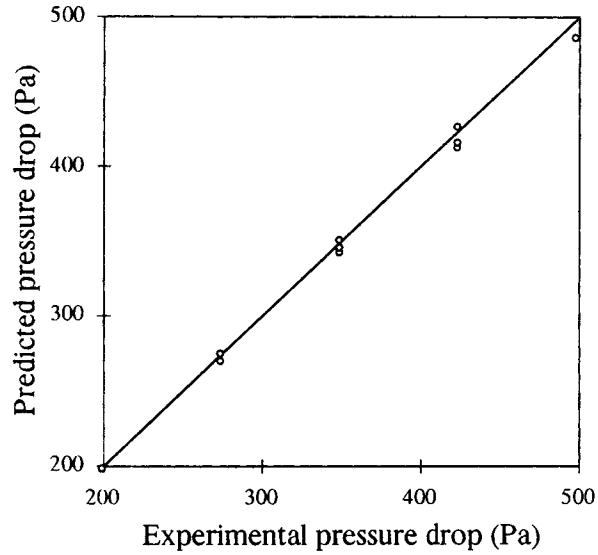

Figure 2a. Predicted vs. experimental values of pressure drop using a calibrated friction factor f_p.

sional as well as three-dimensional predictions have been obtained and compared with experimental data.

Vertical Pneumatic Conveying Hydrodynamics

The validity of the empirical relations concerning interphase friction, pressure drop due to fluid-to-wall frictional forces and the accuracy of the solution algorithm have been checked through one-dimensional predictions. These predictions have been carried out at the same operating conditions used by Hariu and Molstad (1949) and the predicted values have been compared with their experimental data. Figure 1 presents typical predictions of solid volume fraction and phase velocities along

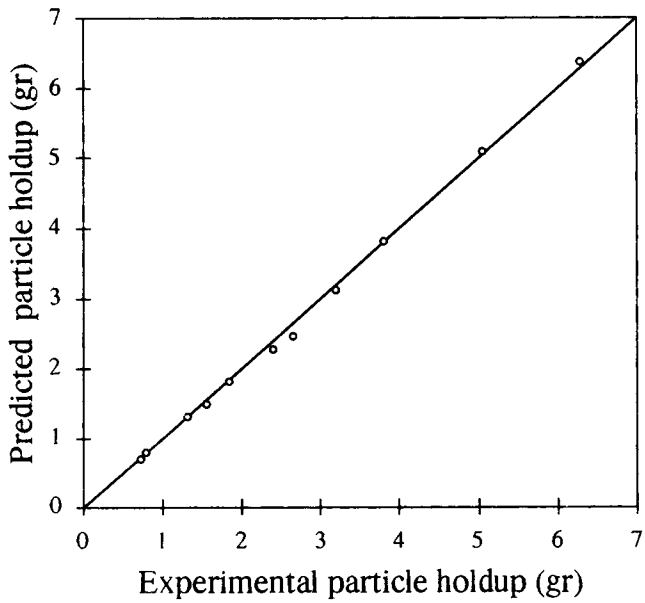

Figure 2b. Predicted vs. experimental values of particle holdup using a calibrated friction factor f_p.

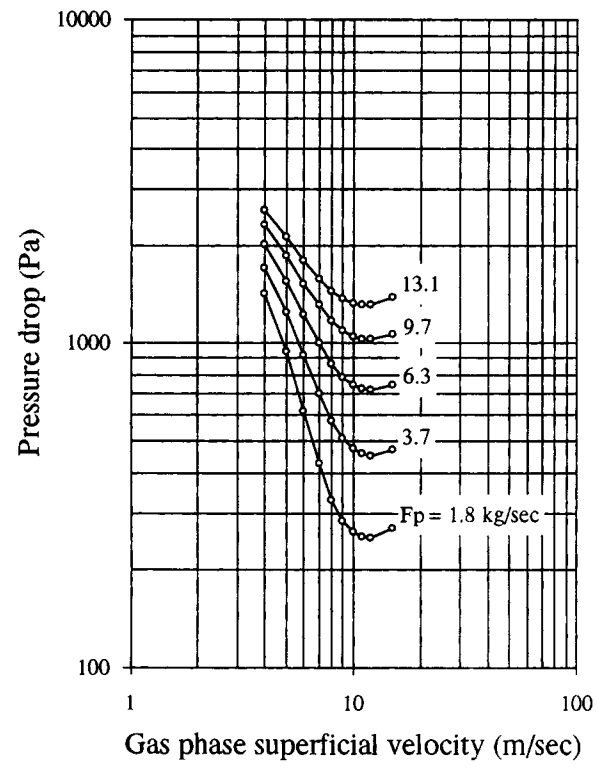

Figure 3. Choking behavior prediction.

the height of a pneumatic conveying lift line. The predictions have been made for particles with 500 μm diameter and 2,600 kg/m^3 density carried by air at a lift line of 1.4 m height and 13.5 mm diameter. The gas velocity decreases as the solids accelerate; the solid volume fraction decreases due to the increase in solid velocity at a constant solid mass flow rate.

The proposed model can predict accurately total pressure drop and total void fraction all over the reactor. Since measurements of local particle concentration in pneumatic conveying are not available, only comparisons of the mean voidage predictions with measurements in a lift line have been made.

Figure 2 presents the comparison of predictions with experimental data of pressure drop and particle holdup for the above mentioned lift line. Predictions have been obtained using a calibration procedure of the hydrodynamics model with reference to experimental data of pressure drop, that can be done through a calibration of the solid-to-wall friction factor, f_p. Figure 3 illustrates the ability of the proposed model to predict the choking behavior of a riser reactor. Predicted values that have been obtained using Zenz's (1949) experimental conditions are in very good agreement with experimental data.

Riser Reactor

Having established the accurate one-dimensional modeling of vertical pneumatic conveying hydrodynamics, three-dimensional predictions have been obtained in order to evaluate heat transfer, chemical reaction and geometry effects, especially at the feed injection area of a riser reactor.

Geometry considered

Figure 4a illustrates the geometry of the considered riser-

reactor, that retains the main features of practical equipment. The catalyst enters from the bottom of the reactor. Feed is injected into the reaction zone through eight nozzles, uniformly spaced along the circumference, at the base of the reactor. The angle between nozzles and the horizontal plane is 60° and zero swirling motion was assumed at inlet.

Operating conditions

The basic operating conditions are:

Hydrocarbons	
Total mass-flow rate	42.7 kg/s
Inlet velocity	50 m/s
Inlet temperature	568 K
Gas-oil concentration at reactor inlet	1.0 kg/kg
Catalyst	
Total mass-flow rate	140 kg/s
Inlet temperature	1,025 K

Physical properties

The physical properties of the fluid mixture are presented below. The properties of the gaseous phase are considered constant and are calculated at a typical operating temperature and pressure and a typical product distribution of a riser reactor.

Hydrocarbons	
Density	7.2 kg/m^3
Laminar viscosity	2×10^{-5} Pa·s
Thermal conductivity	0.07 W/(m·K)
Specific heat (gas)	3,350 J/(kg·K)
Specific heat (liquid)	2,670 J/(kg·K)
Heat of vaporization	191 kJ/kg
Vaporization temperature	698 K
Catalyst	
Particle density	1,300 kg/m^3
Specific heat	1,110 J/(kg·K)
Particle diameter	60 μm

Reaction kinetics data

Reaction kinetics data, the ones proposed by Weekman and Nace (1970), are presented below. The heat of endothermic cracking reaction is 300 kJ/kg of hydrocarbons converted (Mauleon and Courcelle, 1985).

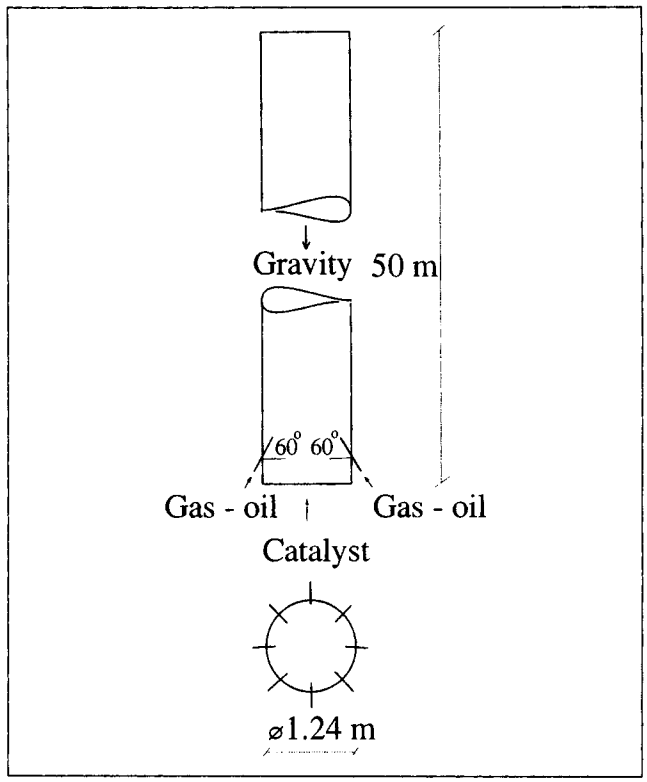

Figure 4a. Geometry considered.

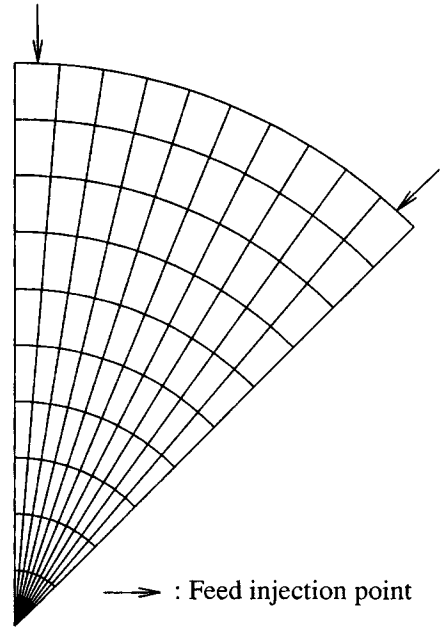

Figure 4b. Computational grid for a cross section of the reactor.

Reaction	Constant (900°F, 482°C)	Activation energy
Gas-oil cracking	$K_0 = 0.266$ h^{-1}	$E_0 = 10$ kcal/mol
Gasoline formation	$K_1 = 0.214$ h^{-1}	
Gasoline cracking	$K_2 = 0.0188$ h^{-1}	$E_2 = 18$ kcal/mol
Catalyst decay	$n = 0.72$	$E_n = -1.7$ kcal/mol

Finite-domain grid

Since the flow pattern repeats itself in every 45° sector of the riser-reactor cross-section, the integration domain is restricted in the θ-direction to only one 45° sector. The computational grid used consists of $10 \times 10 \times 70$ cells in the θ, r and z directions, respectively. A nonuniform grid was used along the z direction. At the base of the reactor, where flow inhomogeneities are significant, 50 computational cells in the z-direction were used for the first 10 m. For the rest 40 m of the reactor, where a plug flow mode is obtained, only 20 cells in the z-direction were used. The grid employed in the θ-r planes is illustrated in Figure 4b.

Boundary conditions

Inlets. At both the hydrocarbon and catalyst inlets appropriate boundary conditions are used to specify the prescribed flow conditions.

Hydrocarbons Inlet

At $z=0$, $r=R$, $\theta=0$ and at $z=0$, $r=R$, $\theta=\pi/4$ (that is, at nozzles' exits)

Mass-flow rate	: F_g	= 42.7/8/2 kg/s	= 2.67 kg/s
Velocity	: w_g	= 50 m/s × sin 60°	= 43.3 m/s
	v_g	= 50 m/s × cos 60°	= 25 m/s
	$(ur)_g$	= 0 m/s	
Specific enthalpy	: h_g	= 0 J/kg (T_{ref} = 568 K)	
Gas-oil concentration	: y_1	= 1 (kg gas-oil/kg feed)	

At $z=0$, $r=[0, R]$, $\theta=[0, \pi/4]$

Mass-flow rate	: F_p	= 140/8 kg/s	= 17.5 kg/s
Specific enthalpy	: h_p	= 1,110 J/(kg·K) × 1,025 K = 1.138×10^6 J/kg (T_{ref} = 0 K)	

Outlet. The external pressure was assumed uniform. As the fluid is assumed incompressible, the external pressure is set equal to zero and the computed pressures are relative to this one.

Walls. At walls, shear stresses are computed from appropriate "wall functions" (Launder and Spalding, 1972). Pressure drop due to gas-to-wall and particles-to-wall frictional forces enter the appropriate momentum equations as additional source/sink terms, as described earlier. It is assumed that there is no heat exchange to the environment, that is, the walls are considered adiabatic.

Computational details

An iterative procedure was used to solve the finite-domain equations. To obtain convergence, relaxation of the false-time step (Markatos, 1989) was required for all velocity variables, while linear relaxation was required for the rest of the dependent variables. The set of the finite-domain equations was solved in two steps. First, the pressure (that is, the overall continuity equation), the six velocity components and the two volume-fraction equations were solved simultaneously over the field. Then, for a calculated flow field, the two enthalpy and the two concentration equations were solved in order to calculate temperature and reaction distributions all over the reactor.

Those two steps were repeated until full convergence for all variables was obtained. The above procedure was followed in order to optimize computational time, since the calculation of the hydrodynamics is three times slower than the calculation of the temperature and concentration distributions. The required computer time is of the order of 4 ms per grid node, per variable and per iteration on an Acorn Archimedes 440/1 personal computer. A total of 250 iterations were required for the convergence of the hydrodynamics, and 100 for the rest of the variables. Thus, a typical run requires 20 h of CPU time, for the grid employed.

Presentation and Discussion of Results

The values of the dependent variables are calculated at the centers of the control volumes all over the reactor considered. The presentation of results is made in the form of velocity vectors and contours of scalar variables at selected planes of the riser reactor.

Figure 5 presents the flow field of both phases at three vertical θ-planes, namely at $\theta=0$, $\theta=\pi/16$ and $\theta=\pi/8$, where θ is the circumferential distance measured from the gas inlet plane. Figure 6 presents the flow field of the gaseous phase at four selected cross-sectional z-planes, namely at $z=0$, $z=0.4$m, $z=0.8$m and $z=1.2$m, where z is the axial distance of the cross-section from the gas inlet plane.

To evaluate the effects of the flow on the temperature distribution and the chemical reaction progress, temperature and yields fractions contours are plotted at the above-mentioned θ- and z-planes. Figure 7 presents the temperature distribution of both phases at the three selected θ-planes, while Figure 8 presents the temperature distribution of hydrocarbons at the four selected z-planes. Figure 9 presents the distribution of cracking products at the three selected θ-planes, while Figures 10 and 11 present the distribution of cracking products at the four selected z-planes. Finally, the mean values of temperature and yields concentrations along the height of the reactor are presented in Figure 12.

Inspection of Figure 5 reveals different flow patterns at different vertical planes that depend on the distance of the plane from the gas inlet plane. At the $\theta=0$ plane the flow field presents large inhomogeneities that tend to dissappear at the $\theta=\pi/16$ and $\theta=\pi/8$ planes. Both phases have almost equal velocities with the exception at the area in the vicinity of the

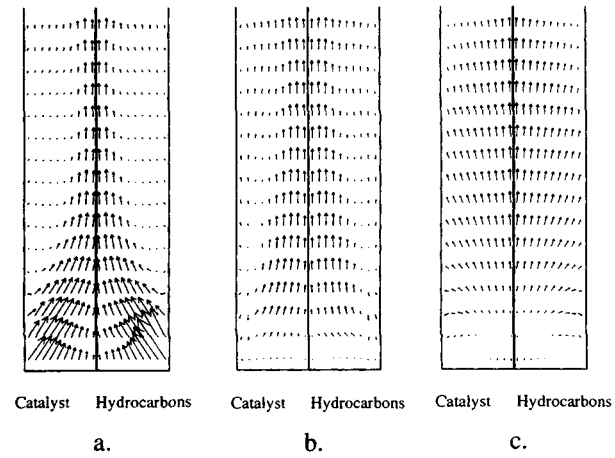

Figure 5. Flow field at vertical planes passing: (a) from the gas inlet point; (b) $\pi/16$ from the gas inlet point; (c) $\pi/8$ from the gas inlet point.

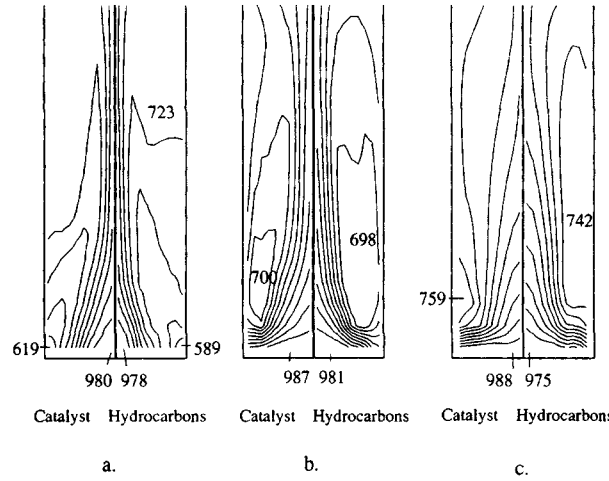

Figure 7. Temperature distribution (K) of catalyst and hydrocarbons at vertical planes passing: (a) from the gas inlet point; (b) $\pi/16$ from the gas inlet point; (c) $\pi/8$ from the gas inlet point.

nozzles, where high interphase slip is calculated. Figure 6 shows that at cross-sections at the base of the reactor, two symmetrical and opposite vortices appear that tend to vanish with height.

The temperature distribution at the injection area of a riser reactor is mainly affected by the feed injection geometry. The feed injector configuration can control the flow pattern and thus eliminate high temperature gradients that lead to overcracking to undesirable products. Figures 7 and 8 illustrate that feed injection effects on temperature distribution can be evaluated by the proposed model. High temperatures are predicted near the axis and especially at the stagnation region at the bottom of the reactor, while low temperatures are predicted near the feed injection nozzles, as expected. Large flow inhomogeneities (Figure 5a) lead to high temperature gradients (Figure 7a), while a more uniform flow pattern (Figure 5c) leads to a more uniform temperature distribution (Figure 7c).

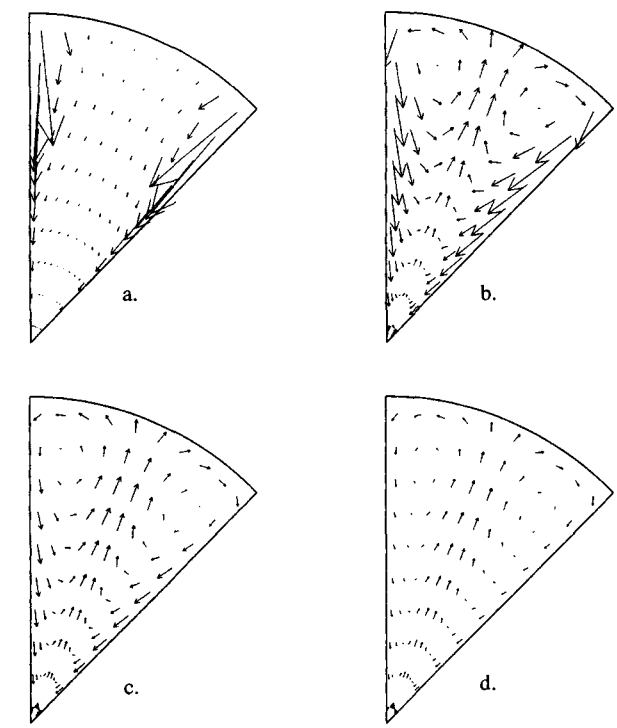

Figure 6. Flow field of the gaseous phase at cross-sectional planes passing: (a) from the gas inlet point; (b) 0.4 m from the gas inlet point; (c) 0.8 m from the gas inlet point; (d) 1.2 m from the gas inlet point.

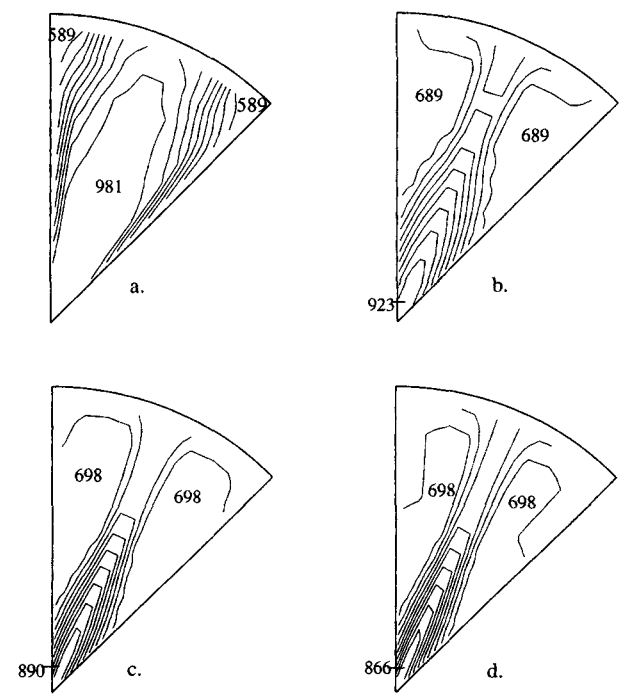

Figure 8. Temperature distribution (K) of the gaseous phase at cross-sectional planes passing: (a) from the gas inlet point; (b) 0.4 m from the gas inlet point; (c) 0.8 m from the gas inlet point; (d) 1.2 m from the gas inlet point.

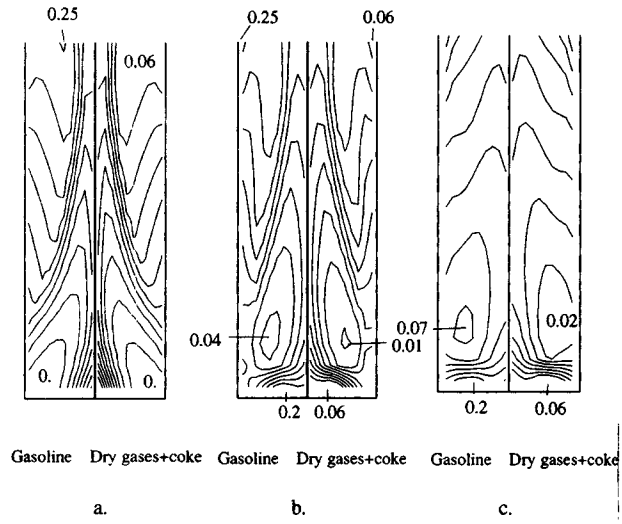

Figure 9. Concentration distribution (w/w) of gasoline and dry gases + coke at vertical planes passing: (a) from the gas inlet point; (b) $\pi/16$ from the gas inlet point; (c) $\pi/8$ from the gas inlet point.

The effects of temperature distribution on the progress of the cracking reactions are presented in Figures 9, 10 and 11. It is reported that at higher temperatures overcracking to undesirable products occurs, while at lower temperatures the cracking reactions are not initiated (Mauleon and Courcelle, 1985); this behavior is predicted by the results obtained.

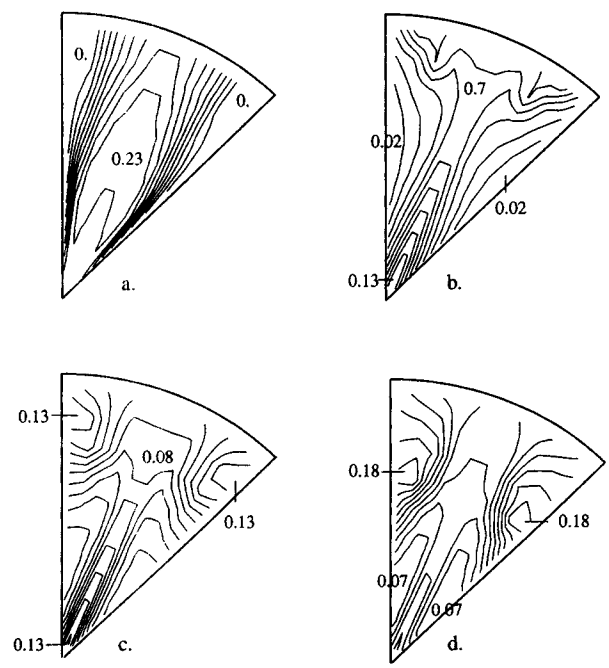

Figure 10. Concentration distribution (w/w) of gasoline at cross-sectional planes passing: (a) from the gas inlet point; (b) 0.4 m from the gas inlet point; (c) 0.8 m from the gas inlet point; (d) 1.2 m from the gas inlet point.

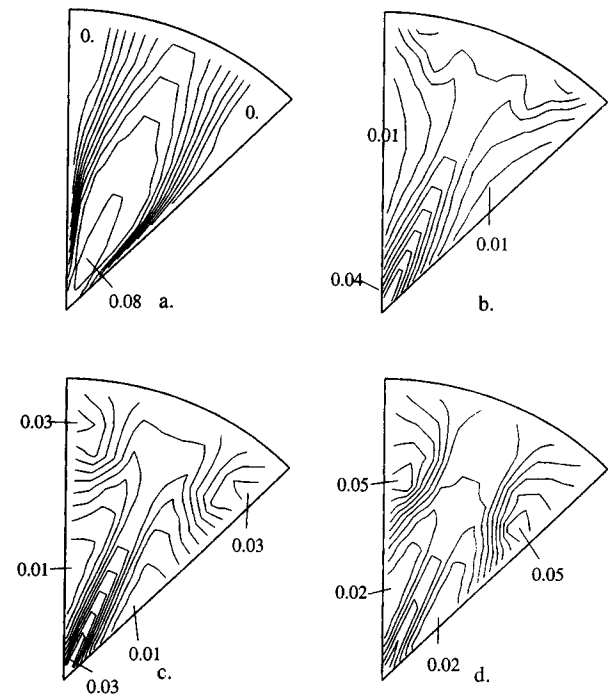

Figure 11. Concentration distribution (w/w) of dry gases + coke at cross-sectional planes passing: (a) from the gas inlet point; (b) 0.4 m from the gas inlet point; (c) 0.8 m from the gas inlet point; (d) 1.2 m from the gas inlet point.

The predicted overall performance of a riser reactor is presented in Figure 12. Figure 12a presents the predicted mean temperatures of both phases along the height of the reactor. The temperatures of both phases become equal at a height of 4m above the feed injection plane; a further decrease in the mixture temperature occurs due to the endothermic cracking reaction. A local minimum in the hydrocarbons temperature distribution is predicted; this is an effect of the feed injection geometry, because the main stream of the "cold" feed does not enter at the base of the reactor, since the feed injectors are located at a 60° angle with the horizontal plane. The predicted temperature distribution along the riser is consistent with reported distributions in industrial riser reactors (Yen et al., 1985). Figure 12b presents the predicted yields concentrations along the riser reactor. The local minimum in concentrations at the bottom of the reactor is also an injection geometry effect. Figure 12c presents the overall performance of the reactor that leads to a 85% conversion and to a 47% gasoline selectivity. A local maximum in gasoline concentration (51% at 30m) is predicted, because above this height the gasoline cracking rate is greater than the gasoline formation rate and thus overcracking to dry gases and coke takes place.

Conclusions

A mathematical model developed predicts the two-phase reacting flow in a catalytic cracking riser reactor. It can be applied to the three-dimensional processes that take place over the feed injection area, the most complex part of a riser reactor. A stable numerical algorithm was used to solve the complete

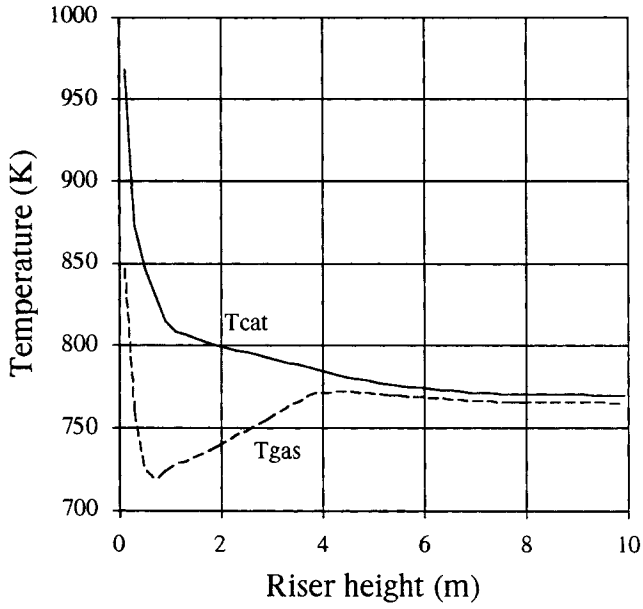

Figure 12a. Temperature vs. riser height (10 m).

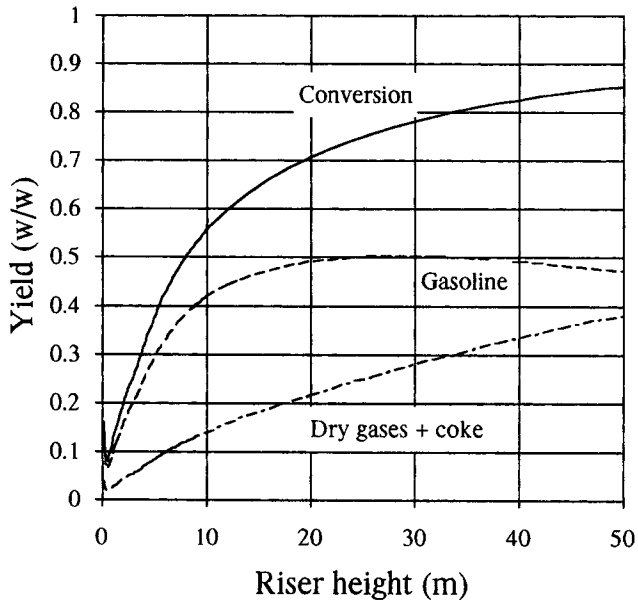

Figure 12c. Yield fractions vs. riser height (50 m).

system of the equations involved. It can predict the most important engineering aspects of a riser catalytic cracking reactor, including pressure drop, catalyst holdup, interphase slip velocity, catalyst acceleration zone, choking behavior and temperature distribution of both phases, and yields distribution all over the reactor. It can also predict geometry effects, especially in the complex feed injection area, where the cracking reactions are initiated. It can also obtain realistic solutions for complex engineering two-phase problems, using modest personal computers and practical computer resources. Future work will include a more realistic kinetics scheme and the calculation of the vaporization of gas oil inside the reactor.

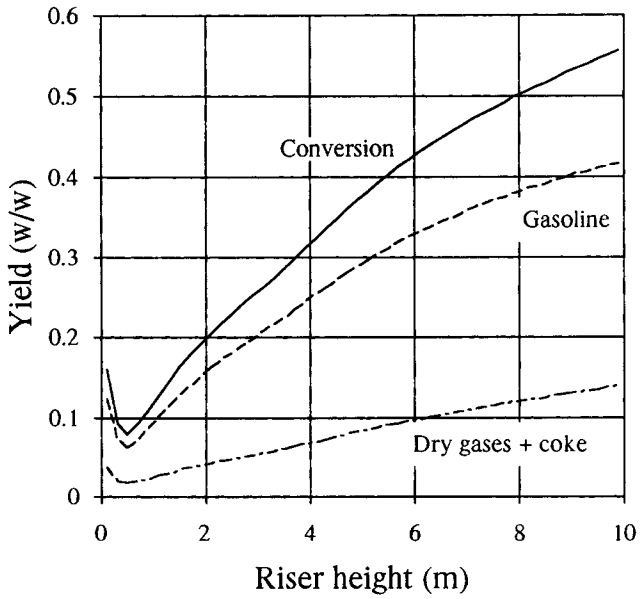

Figure 12b. Yield fractions vs. riser height (10 m).

Acknowledgment

The authors express their thanks to CHAM Ltd., London, for allowing the use of their general computer program PHOENICS.

Notation

A_{pr} = particle projected area per unit volume (m^2/m^3)
C_D = drag coefficient
D = pipe diameter (m)
d_p = particle diameter (m)
f_g = fluid-to-wall friction factor
f_p = particle-to-wall friction factor
g = gravitational acceleration (9.81 m/s)
h = specific enthalpy (J/kg)
h_{pg} = interphase heat-transfer coefficient ($W/m^2 \cdot K$)
k_g = gas thermal conductivity ($W/m \cdot K$)
k_0 = gas-oil cracking constant (h^{-1})
k_1 = gasoline formation constant (h^{-1})
k_2 = gasoline cracking constant (h^{-1})
K_i = $k_i \rho_g / \rho_l$
L = pipe length (m)
n = catalyst decay constant
Nu_p = $(h_{pg} d_p / k_g)$
p = pressure (N/m^2)
q_{pg} = interphase heat-transfer rate per unit volume (W/m^3)
R_i = volume fraction of phase i (vol./vol.)
R_0 = gas-oil cracking rate (kg/s)
R_1 = gasoline formation rate (kg/s)
R_2 = gasoline cracking rate (kg/s)
Re_p = $(d_p \rho_g / \mu_g) | V_g - V_p |$
Re_t = $(d_p \rho_g V_t / \mu_g)$
S_φ = source term per unit volume
t_c = catalyst residence time (h)
V = velocity (m/s)
V_t = terminal (free-fall) velocity (m/s)
u = circumferential velocity (m/s)
v = radial velocity (m/s)
w = axial velocity (m/s)
y_i = concentration of lump i in the gaseous phase (w/w)
y_1 = gas-oil concentration (w/w)
y_2 = gasoline concentration (w/w)

Greek letters

Γ_φ = diffusion coefficient
$\epsilon = R_g$ = lift line voidage
μ = viscosity (Pa·s)
ρ = density (kg/m^3)
φ = dependent variable

Subscripts

p = particulate phase (catalyst)
g = gaseous phase (hydrocarbons)
l = liquid phase (feed)

Literature Cited

Hariu, O. H., and M. C. Molstad, "Pressure Drop in Vertical Tubes in Transport of Solids by Gases," *Ind. Eng. Chem.*, **41**(6), 1148 (1949).

Jacob, S. M., B. Gross, S. E. Voltz, and V. W. Weekman, Jr., "A Lumping and Reaction Scheme for Catalytic Cracking," *AIChE J.*, **22**(4), 701 (1976).

Kunii, D., and O. Levenspiel, *Fluidization Engineering*, Wiley, p. 217 (1969).

Lapple, C. E., "Dust and Mist Collection," *Chemical Engineering Handbook*, 3rd edition, J. H. Perry, ed., McGraw-Hill, New York, p. 1018 (1950).

Launder, B. E., and D. B. Spalding, *Mathematical Models of Turbulence*, Academic Press, London (1972).

Markatos, N. C., and A. Moult, "The Computation of Steady and Unsteady Turbulent, Chemically—Reacting Flows in Axisymmetrical Domains," *Trans. Instn. Chem. Engrs.*, **57**, 156 (1979).

Markatos, N. C., and A. K. Shinghal, "Numerical Analysis of One-dimensional, Two Phase Flow in a Vertical Cylindrical Passage," *Adv. Eng. Software*, **4**(5), 99 (1982).

Markatos, N. C., "The Mathematical Modelling of Turbulent Flows," *Appl. Math. Modelling*, **10**, 190 (June 1986).

Markatos, N. C., "Modelling of Two-Phase Transient Flow and Combustion of Granular Propellants," *Int. J. Multiphase Flow*, **12**(6), 913 (1986).

Markatos, N. C., "Computational Fluid Flow Capabilities and Software," *Ironmaking and Steelmaking*, **16**(4), 266 (1989).

Mauleon, J. L., and J. C. Courcelle, "FCC Heat Balance Critical for Heavy Fuels," *Oil & Gas J.*, 64 (Oct. 21, 1985).

McKetta, J. J., *Encyclopedia of Chemical Processing and Design*, Cracking Catalytic, **Vol. 13**, Marcel Dekker, New York pp. 1-132 (1981).

Patankar, S. V., and D. B. Spalding, "A Calculation Procedure for Heat, Mass and Momentum Transfer in Parabolic Flows," *Int. J. Heat Mass Transfer*, **15**, 1787 (1972).

Richardson, J. F., and W. N. Zaki, "Sedimentation and Fluidization: Part I," *Trans. Inst. Chem. Eng.*, **32**, 35 (1954).

Spalding, D. B., "Turbulent Buoyant Convection," N. Afgan and D. B. Spalding, eds., Hemisphere Publishing, Washington, DC, p. 569 (1977).

Spalding, D. B., *Mathematical Modelling of Fluid Mechanics, Heat Transfer and Chemical Reaction Processes; a lecture course*, Imperial College, London, Rep. HTS/80/1 (1980).

Spalding, D. B., "A General Purpose Computer Program to Multidimensional One or Two-phase Flow," *Mathematics and Computers in Simulation*, **13**, 267 (1981).

Weekman, V. W., and D. M. Nace, "Kinetics of Catalytic Cracking Selectivity in Fixed, Moving and Fluid Bed Reactors," *AIChE J.*, **16**(3), 397 (1970).

Yang, W., "A Correlation for Solid Friction Factor in Vertical Pneumatic Conveying Lines," *AIChE J.*, **24**(3), 548 (1978).

Yen, L. C., R. E. Wrench, and C. M. Kuo, "FCCU Regenerator Temperature Effects Evaluated," *Oil & Gas J.*, 87 (Sept. 16, 1985).

Zenz, F. A., "Two-Phase Fluid-Solid Flow," *Ind. Eng. Chem.*, **41**(12), 2801 (1949).

Manuscript received Aug. 6, 1992, and revision received Nov. 18, 1992.